

**PRELIMINARY REPORT ON SPINEL-RICH CAIs IN AN ANTARCTIC MICROMETEORITE;**Gero Kurat, Naturhistorisches Museum, Postfach 417, A-1040 Vienna, Austria, Peter Hoppe, Physikalisches Institut, Universität Bern, Sidlerstraße 5, CH-3012 Bern, Switzerland, Michel Maurette, Centre de Spectrométrie Nucleaire et de Spectrométrie de Masse, Batiment 108, F-91405 Orsay, France

A large (ca. 330  $\mu\text{m}$ ) micrometeorite (MM) in a polished mount of unmelted Antarctic MMs (92/15, particle 23) consists of a metamorphosed phyllosilicate matrix which includes numerous spinel-rich Ca-Al-rich inclusions and one large chromite grain. The matrix has a clastic texture of Fe- and/or S-rich angular clasts of fine-grained dehydrated phyllosilicates (and others) set into a more Mg, Si-rich matrix. Both major and trace element contents of the MM's matrix, as determined by ASEM, EMP, and SIMS techniques, are chondritic but with depletions in Na, Ca, and Ni, and enrichment in Ba. The spinel-rich CAIs consist of Mg, Al-spinel, which occasionally includes some tiny ( $< 1 \mu\text{m}$ ) perovskite grains, rimmed by an Fe-rich phase whose composition is that of a (probably dehydrated) Fe-rich phyllosilicate. In places, this rim is covered by a Ti-, Al-bearing Ca-rich pyroxene which is fairly Fe-poor (7.8 wt% FeO). Bulk trace element contents of the CAIs are comparable to those of group II CAIs from carbonaceous chondrites. However, some deviations from common group II patterns could indicate more oxidizing conditions during the formation of 92/15-23 CAIs as compared to carbonaceous chondrite CAIs.

**SAMPLE and METHODS.** During January 1991 tens of thousands of dust particles were collected from about 260 t of ice melt-water [1]. Dark colored angular, apparently unmelted, particles were selected from the grain-size fraction 100 - 500  $\mu\text{m}$ , mounted in epoxy, and polished. The collection on polished mount 92/15 contains a large number of partially melted chondritic MMs (scoriaceous MMs), many oxide particles (terrestrial), and also a surprisingly large number of unmelted MMs. The latter comprise mainly coarse-grained crystalline MMs and some phyllosilicate-type MMs. One of these contains abundant CAIs. Because such a micrometeorite was not observed before, it was selected for this study in which we utilized optical microscopy, analytical scanning electron microscopy (ASEM), electron microprobe analysis (EMPA), and secondary ion mass spectrometry (SIMS, modified procedure after [2]).

**RESULTS.** Particle #23 of the mount 92/15 is angular, cut by some cracks and about 330  $\mu\text{m}$  long. The main mass consists of a fine-grained matrix-like material with an inhomogeneous microbreccia texture (Fig. 1). The matrix is Si, Mg-rich (Table 1, 1st analysis) as compared to the lighter-colored clasts, which are Fe- and/or S-rich. The high totals of matrix analyses indicate that it is probably a dehydrated former phyllosilicate matrix. Some very small olivines are present within the matrix as well as some low-Ca pyroxene. The chromite has an aluminous composition. Spinel-rich CAIs are abundant in 92/15-23 (dark grey in Fig. 1). They form round and elongated rounded objects which are mostly continuously covered by a rim (light grey). The rim apparently consists of a single Fe-rich silicate phase whose composition does not correspond to that of olivine. The cation/oxygen ratio (0.7 - 0.73) rather suggests a phyllosilicate but which probably is also dehydrated. On top of the Fe-rich rim there is a discontinuous rim of a Ti, Al-bearing clinopyroxene with a high Mg/Fe ratio. The surface of the particle is covered by a very thin discontinuous magnetite rim (well visible in Fig. 1).

The trace element content of the particle's matrix (Table 2, Fig. 2) is chondritic for all, refractory and volatile, elements. However, all trace elements have somewhat elevated abundances as compared to CI and CM chondrites and Ba is over-abundant by about an order of magnitude. The trace element pattern of the spinel-rich CAI is fractionated among both, the refractory and moderately volatile elements, resembling a group II CAI pattern [4].

**DISCUSSION.** The main mass influx of extraterrestrial matter on the earth consists mainly of dust particles in the size-range 50 - 1000  $\mu\text{m}$  [5]. Of that matter a surprisingly large proportion survives atmospheric entry without melting [6]. Such micrometeorites not only comprise coarse-grained crystalline and anhydrous but also phyllosilicate-dominated lithologies. The latter resemble CI-, CM-, and CR-type mineral-associations [7-10]. Bulk major and trace element abundances in MMs are consistent with that view [11,12] and differences between micrometeorite and chondrite elemental abundances could be shown to be mainly of terrestrial origin(s). The bulk composition of 92/15-23 typically fits that picture. Most elements have abundances comparable to those in CI and CM carbonaceous chondrites. Depletions in MMs in Ni, Ca, and Na are probably due to leaching of soluble phases from the MMs in the terrestrial environment and the enrichment in Ba could be due to atmospheric contamination (compare [11-14]). A similar situation holds for the much smaller IDPs (interplanetary dust particles [13]). Refractory inclusions are characteristic constituents of carbonaceous chondrites. Among MMs such inclusions are apparently rare. Only one fine-grained CAI has been reported so far [16] which has a group I trace element pattern but whose mineralogy is not known. A few CAIs are known from IDPs [17-19]. However, refractory minerals have been reported from many MMs and IDPs.

The spinel-rich CAIs in MM 92/15-23 are the first CAIs from extraterrestrial dust with a group II pattern. Group II CAIs are quite common in CM chondrites [20], a fact which underlines the previously recognized relationship between MMs

## SPINEL-RICH CAIs IN MICROMETEORITE; Kurat G. et al.

and CM chondrites. However, the 92/15-23 CAI has elemental abundances which differ somewhat from those of carbonaceous chondrite CAIs (e.g., [21,22]). Contents of Th, Sc, and V are high in the 93/15-23 CAI (by factors 2, 2, and 10, respectively), and those of Ce and Cr are low. The low abundance of Sr could be a crystal-chemical effect (our CAI is almost pure spinel). All other deviations could indicate a formation of the 92/15-23 CAI in a more oxidizing environment as compared to that of the carbonaceous chondrite CAI formation site. This view is consistent with the higher abundance of pyroxenes and Fe-containing olivines in MMs as compared to carbonaceous chondrites.

**ACKNOWLEDGEMENTS:** This work was financially supported by FWF in Austria (project no. P8125-GEO), the Schweizerische Nationalfonds zur Förderung der wissenschaftlichen Forschung in Switzerland, and by IN2P3 and the European Community SCIENCE (Twining and Operations) Programme (Contract no. SCI-CT91-0618,SSM) in France. We thank Thomas Presper and Franz Brandstätter for performing some of the EDS and EMP analyses.

**REFERENCES.** [1] Maurette M. et al. (1992) *Meteoritics*, 27, 473. [2] Zinner E. and Crozaz G. (1986) *Intl. J. Mass Spectr. Ion Processes*, 69, 17. [3] Anders E. and Grevesse N. (1989) *GCA*, 53, 197. [4] Martin P.M. and Maason B. (1974) *Nature*, 249, 333. [5] Hughes D. W. (1978) In: McDonnell J. A. M. (ed) *Cosmic Dust*, Wiley, 123. [6] Maurette M. et al. (1991) *Nature*, 351, 44. [7] Kurat G. et al. (1992) *LPSC*, XXIII, 747. [8] Christophe Michel-Levy M. and Bourot-Denise M. (1992) *Meteoritics*, 27, 73. [9] Presper T. et al. (1992) *Meteoritics*, 27, 278. [10] Brandstätter et al. (1991) *Eur. J. Mineral. Beih.*, 3/1, 40. [11] Koeberl C. et al. (1992) *LPSC*, XXIII, 709. [12] Kurat G. et al. (1992) *Meteoritics*, 27, 246. [13] Jessberger E. K. et al. (1992) *EPSL*, 112, 91. [14] Presper T. et al. (1993) *LPSCL XXXIV*, 1177. [15] Kurat G. et al. (1993) 18th Symp. *Antarct. Meteorites*, NIPR, Tokyo. [16] Lindstrom D. J. and Klöck A. O. (1992) *Meteoritics*, 27, 243. [17] Zolensky M. E. (1987) *Science*, 237, 1466. [18] McKeegan K. D. (1987) *Science*, 237, 1468. [19] Stadermann F. J. (1991) *LPSC*, XXII, 1311. [20] Ekambaram V. et al. (1984) *GCA*, 48, 2089. [21] Kornacki A. S. and Fegley B. (1986) *EPSL*, 79, 217. [22] Wark D. A. (1986) *EPSL*, 77, 129.

Figure 1: BSE image of spinel-rich CAIs.

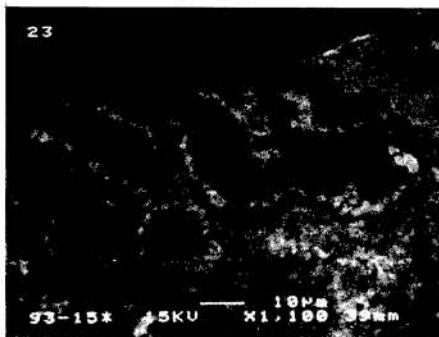


Table 2: MM92/15-23 Ion Probe Data

ppm	Bulk	error	CAI1	error
Li	2.71	0.05	9.8	0.18
K	2175.51	4.57	1313.23	5.81
Sc	26.69	0.24	51.7	0.66
Ti	1429.08	8.03	7754.04	37.38
V	120.67	0.72	445.32	2.73
Cr	6130.64	9.91	1783.09	6.81
Co	1517.9	5.21	302.17	4.24
Sr	18.15	0.3	11.76	0.47
Y	3.91	0.13	2.96	0.23
Zr	17.54	0.48	20	1.01
Nb	1.23	0.12	1.03	0.21
Ba	53.58	0.86	37.27	1.4
Th	0.07	0.04	0.8	0.26
La	0.89	0.08	11.01	0.58
Ce	2.2	0.14	19.56	0.84
Pr	0.37	0.05	4.84	0.37
Nd	1.45	0.11	22.82	0.86
Sm	0.37	0.09	4.3	0.56
Eu	0.08	0.05	0.13	0.1
Gd	0.25	0.13	0.5	0.8
Tb	0.09	0.03	0.35	0.15
Dy	0.62	0.08	1.52	0.29
Ho	0.15	0.04	0.09	0.06
Er	0.33	0.08	0.22	0.12
Tm	0.07	0.02	0.2	0.08
Yb	0.68	0.09	0.82	0.18
Lu	0.05	0.03	0.12	0.09

Figure 2: Orgueil-normalized [3] SIMS data.

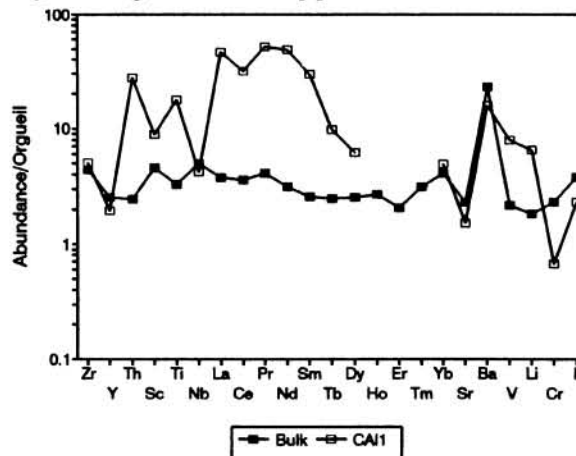


Table 1: MM93/15-23 Phase Compositions (wt%); \*:EDXA normalized to 100%.

	Mx	Mx	Mx	Chr	Px	Sp-rich CAI	Phyl*	Phyl*	Phyl*	Cpx*
						Sp				
SiO <sub>2</sub>	35.30	21.20	24.90	1.14	55.30	0.21	36.10	27.10	30.20	48.90
TiO <sub>2</sub>	0.17	0.18	0.09	0.97	0.13	0.09	0.29	0.35		0.63
Al <sub>2</sub> O <sub>3</sub>	2.10	3.80	5.50	15.80	1.90	70.30	3.40	10.00	4.70	2.56
Cr <sub>2</sub> O <sub>3</sub>	0.56	0.20	0.20	48.40	0.50	0.11	0.43	0.10		0.14
FeO	29.80	42.10	47.20	28.20	12.20	0.83	36.50	46.60	51.30	8.00
MnO	0.57	0.54	0.17	0.31	0.20		0.34	0.69	0.50	0.26
MgO	21.50	13.10	15.20	5.30	29.50	26.00	18.30	14.40	13.10	18.10
NiO	1.39	0.91	0.47				0.43	0.66		
CaO	0.31	0.17	0.07	0.03	0.15		4.20	0.10	0.30	21.40
Na <sub>2</sub> O			0.22							
SO <sub>3</sub>	6.70	17.30	3.40							
Total	98.20	99.50	97.42	98.15	99.88	97.54	99.99	100.00	100.10	99.99

Mx: matrix; Chr: chromite; Px: pyroxene; Sp: spinel;  
Phyl: phyllosilicate; Cpx: clinopyroxene